arXiv:1210.7336v2 [quant-ph] 30 Oct 2012

Single-Spin Addressing Using a Spatially-Varying Dressing Field

Nir Navon, Shlomi Kotler, Nitzan Akerman, Yinnon Glickman, Ido Almog and Roee Ozeri
Department of Physics of Complex Systems, Weizmann Institute of Science, Rehovot 76100, Israel

(Dated: October 31, 2012)

We propose a simple method to spectrally resolve single-spins in a cold atomic system, thus realizing single-spin addressing. This scheme uses a dressing field with a spatially-dependent coupling to the atoms. We realize this scheme experimentally using a linear chain of trapped ions that are separated by $\sim 3\ \mu$m, dressed by a laser field that is resonant with the micromotion sideband of a narrow optical transition.

PACS numbers: 37.10.De; 42.50.Ct; 67.85.-d; 03.67.Mn

In recent years, remarkable capabilities of control and probing of atomic systems have been achieved. Ions and atoms are now routinely imaged at the single-particle level, enabling the study, among other topics, of many-body physics at an unprecedented level of accuracy [1, 2]. For many such applications, single-particle addressing is an increasingly important tool. Early realizations of individual-atom addressing relied on large inter-atomic separations [3, 4], However, applying single-addressing schemes for short inter-particle spacings is very challenging, yet often a necessary task. For example, in order to investigate strongly interacting quantum systems, one has to reduce inter-particle spacings down to near-diffraction-limited distances. Significant experimental efforts have recently been invested in order to develop robust individual-particle addressing schemes with high spatial resolution, both in trapped neutral and ionic systems. Most setups rely on two general approaches: (i) A laser is tightly focused so as to interact only with a single particle, either directly manipulating its quantum state [4, 5]), or inducing a light-shift which spectrally distinguishes the frequency of that atom from the rest [6]. (ii) In analogy with magnetic resonance imaging techniques, a strong gradient in magnetic field is applied in order to Zeeman-shift the atomic levels of interest depending on the position of the particle. Single atoms can be addressed using the transition frequency that matches their location [7–10]. While the first approach is very demanding in term of laser spatial stability and resolution, and becomes difficult when inter-particle spacing compares with the optical wavelength of the addressing setup, the second requires the generation of sufficiently strong magnetic field gradients in order to resolve the frequency separation between transitions in closely-separated particles.

In this letter we propose a simple scheme for single spin addressing in a cold atomic ensemble, that relies on a spatially-dependent dressing field. The resulting dressed eigenstates have spatially-dependent energies and therefore, transitions between dressed states in atoms at different locations are spectrally resolved. We realized this scheme using a linear array of trapped ions. The dressing field was provided by the inhomogenous micromotion of ions in the chain and a narrow linewidth laser that was tuned to the micromotion sideband of a narrow optical quadrupole transition. Quantum information manipulation using microwave-dressed ion qubits has been previously demonstrated in [11].

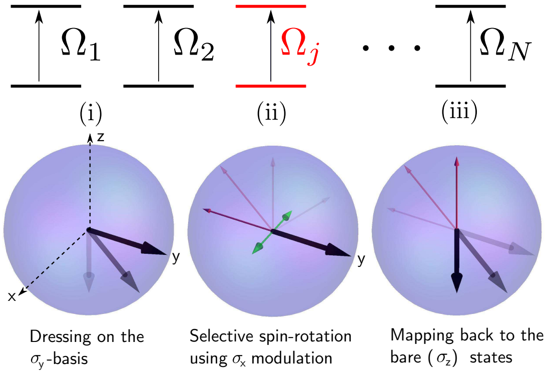
Ω_1
Ω_2
Ω_j
Ω_N
(i)
(ii)
(iii)
z
y
x
y
Dressing on the σ_y-basis
Selective spin-rotation using σ_x modulation
Mapping back to the bare (σ_z) states

FIG. 1: (Color online) The system considered is an array of N identical non-interacting two-level systems, subjected to an external coupling field with a Rabi frequency Ω_j for particle j. The lower panel shows a sketch of the single-spin addressing protocol, involving three steps: (i) the bare eigenstate of all particles ↑ and ↓ at the Bloch sphere poles are mapped onto the dressed eigenstates in the sphere equatorial plane (shown by thick black arrows). (ii) A driving field (shown by the green arrow) which is amplitude-modulated at a frequency Ω_j rotates the spin of particle j (shown by the thin red arrow, and the red two-level system in the upper panel). (iii) The dressed states are mapped back on the bare basis at the sphere poles. All particles end up in state ↓, except particle j which is in ↑.

Different techniques for using the spatial variation of micromotion in ion traps for the purpose of individual addressing have been suggested and demonstrated [12, 13]. Here, we consider a non-interacting array of N two-level systems that are held at fixed positions. The Hamiltonian for particle j is $H^{(j)}_{\rm lab} = H^{(j)}_0 + H^{(j)}_{\rm int}$, where $H^{(j)}_0 = -\frac{\hbar\omega_0}{2}\sigma^{(j)}_z$, σ_z the z-Pauli matrix, and $H^{(j)}_{\rm int}$ is the interaction Hamiltonian between the atom and the laser field, $H_{\text{int}}^{(j)} = \hbar\Omega_j \cos(kx_j - \omega_L t)\sigma_y^{(j)}$, where ω_L is the frequency of the laser field, and k, its wavenumber. Note that while the transition energy $\hbar\omega_0$ is assumed equal for all particles, the Rabi frequency associated with this coupling Ω_j is particle-dependent. In the rotating-wave approximation (RWA) and assuming the Lamb-Dicke regime, the Hamiltonian in the interaction picture reads [14],

$$H_{\text{dress}}^0 = \sum_j \frac{\hbar\Omega_j}{2}\sigma_y^{(j)}, \tag{1}$$

where the frequency of the laser is tuned to the atomic transition $\omega_L = \omega_0$. In order to individually address particle n, we note that H_{dress}^0 is formally equivalent to the Hamiltonian of an array of spin-1/2 in a fictitious magnetic field gradient, in the y-basis. In other words, the two-level systems are coupled to a spatially varying dressing field, and the energies of the dressed states, which are the eigenstates of $\sigma_y^{(j)}$, are position-dependent.

This analogy enables to construct a simple protocol for individual spin rotations, as is illustrated in Fig.1: (i) The bare spin eigenstates (σ_z basis) are mapped onto an eigenstate of the dressed spin (σ_y basis) $|\uparrow\rangle_d/|\downarrow\rangle_d$, and the strong resonant dressing field is turned on, locking the eigenstates in place by opening an energy gap between them. This energy gap is determined by the local coupling strength of each atom to the dressing field. (ii) A small σ_x perturbation is amplitude-modulated (in the ω_0-rotating frame), with a modulation frequency δ, so that the Hamiltonian becomes $H_{\text{dress}} = H_{\text{dress}}^0 + \sum_{j=1}^N \hbar\lambda_j \cos(\delta t)\sigma_x^{(j)}$. This Hamiltonian is solved for each particle n by performing an additional change to a rotating frame, at an angular frequency Ω_n, assuming $\lambda_j, |\delta - \Omega_j| \ll \delta$, and neglecting the counter-rotating terms in this frame of reference [15, 16]. In that case, we readily find that the probability for spin j to be $|\uparrow\rangle_d$, while all the others are $|\downarrow\rangle_d$ is

$$P(t) = P_j(t)\prod_{l\neq j}(1 - P_l(t)), \tag{2}$$

where $P_i(t) = ((\lambda_i/4\bar{\Omega}_i)^2 \sin^2(\bar{\Omega}_i t/2)$ is the Rabi precession, at a frequency $\bar{\Omega}_i = \sqrt{\Delta_i^2 + \lambda_i^2/4}$ and the detuning in the Ω_i-rotating frame is $\Delta_i = \delta - \Omega_i$. For all Ω_j's different from δ, the spins remain locked on y-axis while the spin of particle n is resonantly rotated around the x-axis. (iii) The dressed states are mapped back to the σ_z bare basis. Following this procedure, all particles remain in their initial state except for particle n, whose spin has been rotated.

We experimentally demonstrated the above individual spin-addressing scheme using a chain of atomic ions, held in a linear Paul trap, and typically separated by ~ 3 μm. The experimental setup is presented in detail elsewhere [17]. In short, we trapped and Doppler-cooled one or more ^{88}Sr$^+$ ions in a linear Paul trap. We implemented a two-level system using the $5S_{1/2,+1/2}$ state, hereafter referred to as the bright state, due its photon statistics during state-selective fluorescence detection [18], and the long-lived $4D_{5/2,+3/2}$ state, hereafter called dark state. These two states are connected by an optical, electric-quadrupole, transition at 674 nm. This transition is driven using a narrow-linewidth diode laser stabilized to an external high-finesse cavity [18]. In an ideal linear Paul trap, the micromotion, due to the ac-field modulated on the RF electrodes, vanishes along the symmetry axis of the trap. However, rather than a line of nulled RF amplitude as in the ideal case, the boundary conditions imposed by the trap end-caps generate a linearly increasing RF amplitude around a null-amplitude point at the trap center [19]. The inhomogenity of this excess micromotion along the chain is used as a spatially-dependent coupling of the ions to the laser field. When operating the laser on the micromotion sideband of the quadrupole transition, located at a detuning of $\Omega_{\text{RF}} = 21.75$ MHz from the carrier transition, the resulting Rabi frequency depends on the ion micromotion amplitude via: $\Omega_j = \Omega_c J_1(\eta_j)$, where Ω_c is the carrier Rabi frequency, in the absence of modulation, J_1 is the first-order Bessel function of the first kind [20]. The parameter $\eta_j = \mathbf{k}\cdot\mathbf{x}_j$ is the micromotion Lambe-Dicke parameter of particle j along the laser wavevector $\mathbf{k}$, and $\mathbf{x}_j$ is its micromotion amplitude. For micromotion amplitudes small compared with the transition wavelength, $\eta_j \ll 1$, the local Rabi frequency can be approximated by $\Omega_j \approx \eta_j.\Omega_c/2$. The micromotion amplitude of the ions in the chain can be controlled by applying a differential voltage to the trap end-caps and displacing the ions along the trap axis, or by varying the RF voltage on the trap electrodes.

The values of the dressed state energies $\hbar\Omega_j$ for the different ions was first calibrated. The strength of the dressing field was measured through the frequency of the Rabi oscillations on the micromotion sideband for different end-cap voltages. For multi-spin systems, the population of ions in the dark state was estimated from photon detection histograms. Fig.2a shows the fraction of ions in the dark state versus the micromotion sideband pulse time, for a three-ion chain. The different Rabi frequencies involved can be conveniently extracted by Fourier analysis of the Rabi nutation curve, as shown in Fig.2b. Three frequencies, differing by roughly 5 kHz are clearly observed. In Fig.2c, such spectra are shown as columns as a function of the global axial displacement of the chain. As seen, the three frequencies shift linearly with the displacement. This shows negligible effect of the spatial inhomogeneity of the laser beam profile on the dressed state energies on the length scales of Fig.2. One frequency nulls every time one ion sits on the RF-null (points labeled 1

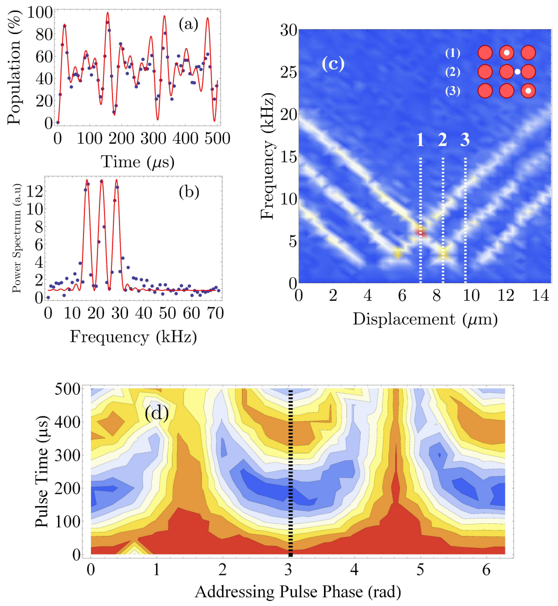

FIG. 2: (Color online) Calibration of the single-spin addressing protocol. (a) and (b) show the time evolution, and Fourier spectrum respectively of the fraction of dark ions in the three-ion chain driven on the micromotion sideband, for a given axial position of the chain. (c) Calibration of the dressed state energies by Fourier transform of the Rabi nutation curve on the micromotion sideband as a function of the axial displacement. The three particular points on the map (labelled 1 to 3) correspond to the RF-null being respectively on the central ion, in between two right-most ions and on the right-most ion, as shown in the schematic drawing on top of the map. The ions (RF-null) are represented by red (white) disks. (d) 2D scan of the phase of the amplitude-modulated driving field (with respect to the dressing beam phase) and the pulse time for a single ion. A σ_x modulation is obtained for a phase $\phi \approx 3.03$ rad (vertical dashed black line).

and 3 on Fig.2c).

In order to apply this scheme to a multi-spin system, one has to address simultaneously all spins for the steps (i) and (iii). This can be solved in two different ways. (1) If micromotion is sufficiently weak so that the carrier Rabi frequency is almost constant throughout the chain, then one can apply a collective carrier $\pi/2$-pulse (along σ_x) to bring the spins to the equatorial plane. Here, the carrier and the micromotion sideband transitions, together with the RF signal for the trap electrodes must all be phase-locked. (2) The spins are set on the equatorial plane using Rapid Adiabatic Passage (RAP) on the micromotion sideband interrupted on resonance. The RAP beam is kept on resonance, and thus automatically dresses the spins. In both schemes, following initialization, a AM-σ_x pulse rotates the spin of the particle of interest. After the single-spin rotation the dressed states are mapped back to the bare states by reversing step (i). While we have successfully implemented both methods, we preferred the former, since RAP is several times slower than the carrier $\pi/2$-pulses.

The amplitude-modulated σ_x field was generated by adding a radio-frequency, that was amplitude-modulated at a frequency δ, to the laser acousto-optic modulator (AOM). This signal had the same carrier frequency and is phase-shifted by $\pi/2$ from the dressing signal. Since the σ_y-dressing and the σ_x driving field were provided by the same beam, then $\lambda_i = \alpha\Omega_i$, and the Rabi frequency $\bar{\Omega}_i$ is proportional to Ω_i when the detuning Δ_i vanishes. The phase of the driving field was tuned in the following way: after the spins are dressed, the phase and time of the modulation are scanned, while the driving frequency δ is tuned to a single-spin resonance. The resulting spin-flip probability for a single ion is displayed in Fig.2d. The period of the pattern is π and we observed that at phases ϕ' and $\phi' + \pi$ (where $\phi' \approx 1.46$) the scan is independent of time, corresponding to a modulation colinear with the dressing field ($\phi = \pm y$). At phases $\phi' \pm \pi/2$ (vertical dashed line in Fig.2d), we observe the highest contrast for the oscillations, corresponding to resonant σ_x rotations of the dressed state. Note that the sum of the σ_y-dressing and the σ_x-modulation could be equally well produced by direct frequency modulation of the σ_y beam.

We next scanned the frequency of the driving field 400 μs pulse. A typical spectrum, displayed in Fig.3a, exhibits three spectral features, corresponding to each ion addressed separately. The spectral splitting of the ions is given by the gradient of the coupling field, which in this case is proportional to the voltage applied on the RF electrodes. Using normal operation voltages, one reaches easily several kHz separation. This is an important figure of merit since small splittings require correspondingly longer pulses in order to frequency-resolve the peaks. Comparing to the method of individual addressing using magnetic field gradients [8, 9], the maximum splitting that we reached, of about 10 kHz, corresponds to a magnetic field gradient of about 50 G/cm (assuming a magnetic field sensitivity of 2.8 MHz/G), which is similar to the one obtained in [9]. The Rabi frequency for each ion is easily deduced from a spectrum such as Fig.3a, taken with a different pulse time. Such a 2D scan is displayed in Fig.3b. We observe that the π-time of all ions are inversely proportional to their addressing frequency, since $\lambda_j = \alpha\Omega_j$, we have $t_\pi^{(j)} = \pi/(\alpha\Omega_j)$ (dashed black hyperbolas). Using the first ion frequency and its corresponding π-time as the only fitting parameters (the splitting for the trap parameters being deduced from an independent measurement as in Fig.2c), we calculated the map showed in Fig.3c, which agrees reasonably well with the experimental data. For the 4 kHz splitting shown in Fig.3a, a π-pulse of respectively 200, 280 and

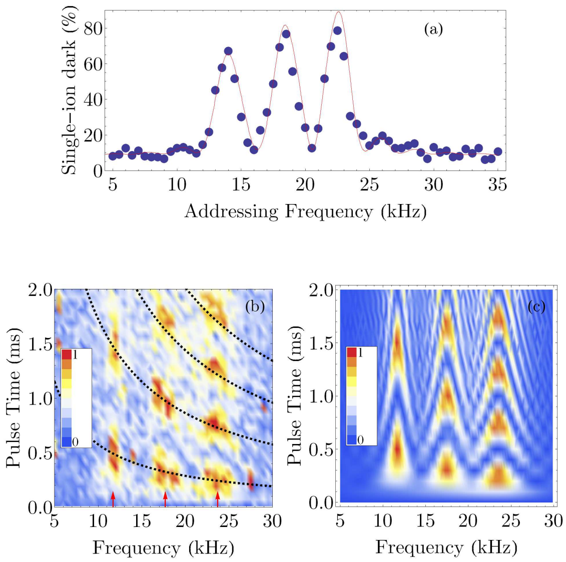

FIG. 3: (Color online) Spectra of the single-addressing protocol. (a): Spectrum for a three-ion chain taken after a pulse time of 400 μs, in a trap whose secular frequencies were $(\omega_x, \omega_y, \omega_z) = 2\pi \times (2.57, 2.45, 1.68)$ MHz. The RF frequency of the trap was 21.75 MHz. (b) and (c) Experimental and theoretical spectra taken for various driving pulse times. Every row in (b) is a similar spectrum to (a). The different Rabi frequencies for each ion are evident. The red arrows mark the different resonances of different ions. The color bar refers to the probability of having one and only one dark ion.

560 μs leads to a spurious excitation of adjacent ions, which results from the overlap of their spectral response. The total crosstalk error, defined as the probability of preparing the whole chain in a different state than the desired one is estimated from Eq.(2) to be respectively 1.6,1.1 and 4.1 % when addressing each ion respectively. The addressing fidelities of 90(2),88(2),85.6(2.5) % are consistent with an additional state preparation error per ion of 4 %, due to the spin-lock efficiency limited at long holding times. This is also consistent with the fidelity reached in a two-ion chain, of 94(2) % (with π-time of 180 μs). This limitation is not fundamental, and could be mitigated by increasing the power in the dressing field, or equivalently by increasing the RF voltage, both of which would increase the frequency gradient, and allow for shorter σ_x operations.

Lastly, we verify the spatially-selective nature of this protocol by taking images on an Electron Multiplying Charge Coupled Device (EMCCD) camera. In the upper panel of Fig.4, we show an image of a three-ion chain, where all the ions are in the bright state. We then selectively flip each ion spin using the above protocol, and average over 50 images. We indeed observe successful single-spin addressing. The faint "ghost" images of adjacent ions are due to errors (see caption of Fig.4).

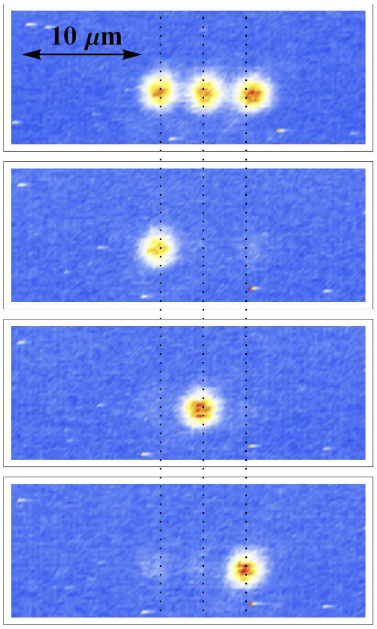

FIG. 4: (Color online) Imaging the single-spin addressing protocol on a three-ion chain. Each image below is an average of 50 pictures taking on an EMCCD camera, with an exposure time of 20 ms. In the upper image, all three ions are in the S state, and therefore fluoresce. In the lower images a single ion remained in the S state while the other two were transferred to the D (dark) state. Because of the long exposure time required for the EMCCD imaging, there is a significant amount of error due to the finite lifetime of the dark state, in addition to the crosstalk errors. For instance on the second image, the error is respectively 7(4) % and 12(5) % for the central and rightmost ion respectively.

To conclude, the method described above is general, not limited to small systems, and relies on single-spin operations only. It allows the generation of any product state of single-qubit operations, and can in principle be adapted to various quantum systems. With trapped ions, this scheme is well suited to address single ions in quantum registers using the typical intrinsic inhomogeneity of micromotion in RF Paul traps and without any additional elements or any need for optical resolution. Our method could be useful with continuous density distributions as well, to select atoms with respect to their coupling to some external field. In particular, atoms with a narrow-line transition, such as neutral Sr or Yb, could be addressed with a sub-wavelength resolution, using the spatial inhomogeneity of the beam itself. Similarly, our technique could be readily useful in atomic fountain clocks to select atoms according to their coupling in the preparation/interrogation microwave cavities, where the inhomogeneities arise from the microwave spatial mode, and would provide an additional knob to study collisional or cavity phase shifts in these clocks.

During the preparation of this manuscript, we became aware of a related work, realizing individual-ion addressing of a two-qubit chain using microwave field gradients on a microfabricated trap [21].

We thank D. Leibfried and N. Davidson for helpful comments on the manuscript, and C. Salomon for fruitful discussions. This research was supported by the Israeli Science Foundation, the Minerva Foundation, the German-Israeli Foundation for Scientific Research, the Crown Photonics Center, the Wolfson Family Charitable Trust, Yeda-Sela Center for Basic Research, and David Dickstein of France.

[1] R. Blatt and C. Roos, Nat. Phys. **8**, 277 (2012).
[2] I. Bloch, J. Dalibard, and W. Zwerger, Rev. Mod. Phys. **80**, 885 (2008).
[3] R. Scheunemann, F. Cataliotti, T. Hänsch, and M. Weitz, Phys. Rev. A **62**, 051801 (2000).
[4] R. Dumke, M. Volk, T. Müther, F. Buchkremer, G. Birkl, and W. Ertmer, Phys. Rev. Lett. **89**, 97903 (2002).
[5] H. Nagerl, D. Leibfried, H. Rohde, G. Thalhammer, J. Eschner, F. Schmidt-Kaler, and R. Blatt, Phys. Rev. A **60**, 145 (1999).
[6] C. Weitenberg, M. Endres, J. Sherson, M. Cheneau, P. Schauß, T. Fukuhara, I. Bloch, and S. Kuhr, Nature **471**, 319 (2011).
[7] D. Schrader, I. Dotsenko, M. Khudaverdyan, Y. Miroshnychenko, A. Rauschenbeutel, and D. Meschede, Phys. Rev. Lett. **93**, 150501 (2004).
[8] S. Wang, J. Labaziewicz, Y. Ge, R. Shewmon, and I. Chuang, App. Phys. Lett. **94**, 094103 (2009).
[9] M. Johanning, A. Braun, N. Timoney, V. Elman, W. Neuhauser, and C. Wunderlich, Phys. Rev. Lett. **102**, 73004 (2009).
[10] N. Brahms, T. Purdy, D. Brooks, T. Botter, and D. Stamper-Kurn, Nat. Phys. **7**, 604 (2011).
[11] N. Timoney, I. Baumgart, M. Johanning, A. Varon, M. Plenio, A. Retzker, and C. Wunderlich, Nature **476**, 185 (2011).
[12] Q. Turchette, C. Wood, B. King, C. Myatt, D. Leibfried, W. Itano, C. Monroe, and D. Wineland, Phys. Rev. Lett. **81**, 3631 (1998).
[13] D. Leibfried, Phys. Rev. A **60**, 3335 (1999).
[14] D. Leibfried, R. Blatt, C. Monroe, and D. Wineland, Rev. Mod. Phys. **75**, 281 (2003).
[15] B. Thimmel, P. Nalbach, and O. Terzidis, Euro. Phys. J. B **9**, 207 (1999).
[16] In the second RWA, all frequencies are of the same order of magnitude (in the kHz range), and one can thus expect some breakdown of the RWA.
[17] N. Akerman, Y. Glickman, S. Kotler, A. Keselman, and R. Ozeri, App. Phys. B pp. 1–8 (2011).
[18] A. Keselman, Y. Glickman, N. Akerman, S. Kotler, and R. Ozeri, New J. Phys. **13**, 073027 (2011).
[19] D. Berkeland, J. Miller, J. Bergquist, W. Itano, and D. Wineland, J. App. Phys. **83**, 5025 (1998).
[20] D. Wineland and W. Itano, Phys. Rev. A **20**, 1521 (1979).
[21] U. Warring, C. Ospelkaus, Y. Colombe, R. Jordens, D. Leibfried, and D. Wineland, arXiv:1210.6407 (2012).